Laser and Particle Beams (2008), *26*, 537–543. Printed in the USA.

doi:10.1017/S0263034608000578

Physical processes in laser interaction with porous low-density materials

N.G. BORISENKO,[2] A.E. BUGROV,[1] I.N. BURDONSKIY,[1] I.K. FASAKHOV,[1] V.V. GAVRILOV,[1] A.YU. GOLTSOV,[1] A.I. GROMOV,[2] A.M. KHALENKOV,[2] N.G. KOVALSKII,[1] YU.A. MERKULIEV,[2] V.M. PETRYAKOV,[1] M.V. PUTILIN,[1] G.M. YANKOVSKII,[1] AND E.V. ZHUZHUKALO[1]

[1]Troitsk Institute for Innovation and Fusion Research, Troitsk, Moscow, Russia
[2]P.N. Lebedev Physical Institute of RAS, Moscow, Russia

(RECEIVED 6 March 2008; ACCEPTED 24 July 2008)

Abstract

New results obtained in experiments on laser irradiation ($I = 5 \times 10^{13}$ W/cm^2, $\lambda = 1.054$ μm) of low-density (2–10 mg/cm^3) porous materials (agar, triacetate cellulose, and foam polysterene) are presented and discussed from the standpoint of optimum porous material utilization in target designs for inertial confinement fusion. The influence of low-density material microstructure of irradiated samples on the absorption of laser radiation and the energy transfer processes was investigated using X-ray and optical diagnostic methods with high temporal and spatial resolution.

Keywords: Energy transfer; High-intensity laser pulses; Inertial confinement fusion; Laser-plasma interaction; Low-density porous material; Plasma hydrodynamics

INTRODUCTION

A study of laser light interaction with low-density (1–100 mg/cm^3) porous media is of great interest in that it provides the possibility for solving a number of important scientific and technical problems, since the use of porous materials in various types of irradiated targets is believed to be a fruitful and promising approach. First of all, utilization of low-density porous materials as a component of advanced targets in inertial confinement fusion (ICF) should be noted. These materials can provide the uniform energy deposition to the targets in direct-drive ICF, as well as the suppression of high-Z plasma expansion, and thus stabilization of X-ray conversion regions in indirect-drive ICF (Lindl, 1995; Hoffmann *et al.*, 2005; Jungwirth, 2005; Hora, 2007; Vatulin *et al.*, 2004; Mulser *et al.*, 2004). Target design for "greenhouse" ICF concept (Gus'kov *et al.*, 1995) should also be mentioned. Application of low-density media seems to be helpful and promising in many other (non-ICF) research programs including development of powerful coherent and incoherent X-ray sources (Landen *et al.*, 2001; Schollmeier *et al.*, 2006; Riley *et al.*, 2007), laboratory modeling of astrophysical objects and phenomena (Drake *et al.*, 2000), EOS investigations in conditions of extremely high energy densities in different materials (Koenig *et al.*, 1999).

On the "Mishen" facility (Troitsk Institute for Innovation and Fusion Research, Moscow, Russia) for several years the experiments on laser irradiation of targets on the base of agar-agar (thin organic fibers and films randomly distributed over the sample volume) were conducted at the laser power densities at the range of 10^{13}–10^{14} W/cm^2. Laser light absorption and scattering, plasma production and homogenization, energy transfer and X-ray conversion were investigated (Bugrov *et al.*, 1997, 1999*a*, 1999*b*, 2000, 2001, 2002, 2003, 2006; Gavrilov *et al.*, 2004). Recently, the technology of low-density target fabrication on the base of cellulose triacetate (TAC) and foam polystyrene was elaborated at the P.N. Lebedev Physical Institute of the Russian Academy of Sciences (Gromov, 1999; Borisenko, 2003; Koresheva *et al.*, 2005; Khalenkov *et al.*, 2006). Microstructures of agar and TAC are very similar ("open cells" structure), but characteristic sizes of structural elements and cells in TAC are by an order of magnitude smaller than those in agar. Typical thickness of fibers/films in agar and TAC samples are equal to several micrometers and several tenths of micrometer, correspondingly.

Address correspondence and reprint requests to: V.V. Gavrilov, Troitsk Institute for Innovation and Fusion Research, Troitsk, Moscow, Russia. E-mail: vvgavril@triniti.ru

Cellular foam-like microstructure of polystyrene ("closed cells" structure) differs strongly from microstructure of agar and TAC. To choose the porous material and its optimal parameters for the use in constructions in different versions direct and indirect ICF targets it is necessary to investigate in detail the processes of laser light absorption and energy transfer inside irradiated samples. The goal of this paper is the comparative investigation of the physical processes in laser-irradiated porous samples of different microstructure.

STATEMENT OF EXPERIMENTS AND DIAGNOSTIC TECHNIQUES

In the direct-drive concept of laser-initiated ICF, a low-density porous material deposited on the spherical target surface can smooth ablation pressure nonuniformities imprinted by irregularities in laser illumination. It was shown in our previous papers that as the result of efficient lateral and longitudinal energy transport in laser-irradiated low-density porous media, the sufficiently uniform pressure distribution is realized over the comparatively large area on the rear side of the used agar samples. The pressure as high as 1 Mbar was estimated over the area with diameter by a factor of three larger than that of the focal spot in experiments on irradiation 500 μm-thick agar samples of the 2 mg/cm^3 average density. The obtained experimental data confirm our predictions that low-density materials provide the efficient smoothing of irradiation nonuniformities and can be successfully used in designs of advanced ICF targets (Bugrov *et al.*, 2001).

In the present indirect-drive ICF target designs, the expansion of high-Z plasma produced at the laser-illuminated inner surface of hollow cylindrical shell hohlraum (X-ray converter) is suppressed by filling the hohlraum with a low-Z gas. This method brings with it a number of scientific and technical problems (Lindl, 1995). The utilization of low-density porous matter could be an alternative approach for solving the problem of high-Z plasma expansion. We conducted a set of experiments on suppression of medium- and high-Z plasma expansion by the agar layers of different average density and thickness deposited onto the plane Ni foils modeling the hohlraum wall. One of the main results of these experiments was the following: the 200–300 μm thick agar layer with an average density of 2–3 mg/cm^3 deposited on laser irradiated targets of medium- or high-Z elements suppresses efficiently the expansion of X-ray emitting plasma (Bugrov *et al.*, 2003). The intensity of soft X-rays is about 50% of that measured without agar covering, and it increases up to 70% when agar is doped with $CuCl_2$.

We are going to carry out the experiments with TAC and foam polysterene targets similar to those which have been realized with agar samples. And first of all, it is necessary to investigate the processes of laser light absorption and energy transport in laser-irradiated TAC and polystyrene samples, and to compare the obtained data with those obtained in experiments with agar targets.

The experiments were carried out on the "Mishen" facility (Nd-glass laser with an output beam energy $E = 50–100$ J at $\lambda = 1.054$ μm in 3 ns pulse. Planar agar $(C_{12}H_{18}O_9)_n$, TAC $(C_{11}H_{16}O_8)_n$ aerogel, and foam polystyrene $(CH)_n$ targets were irradiated. In most experiments, the average intensity within a focal spot ~250 μm diameter was $\sim 5 \times 10^{13}$ W/cm^2. The average density of 0.2–0.6 mm-thick samples was varied in the range of 2–10 mg/cm^3. Thin Al foils were disposed at the rear surface of the low-density porous samples. The structures of cellulose triacetate (Khalenkov *et al.*, 2006) and agar (thin organic fibers and films randomly distributed over the sample volume, so called "open cells" structure), as well as foam polystyrene (quasi-regular distribution of "closed cells") are shown in Figure 1.

The following diagnostics were used in these experiments: multiframe side-on optical shadowgraphy of accelerated matter at the target rear side; streak camera recording of the luminosity in visible at the rear surface of irradiated targets; X-ray streak camera side-on recording of plasma emission; X-ray imaging of hot plasma region with filtered pinhole cameras. Detailed description of the used diagnostic methods with estimations of measurement accuracy can be found in our earlier papers (Burdonskiy *et al.*, 1988; Bolotin *et al.*, 1992; Bugrov *et al.*, 1999*b*).

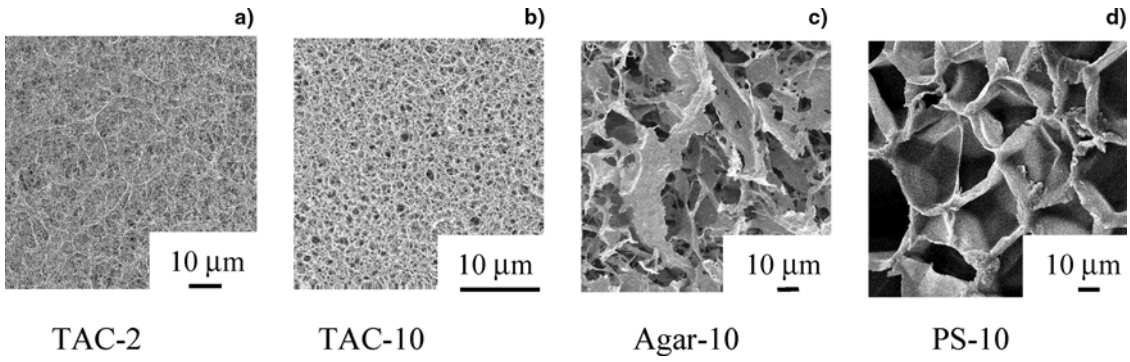

Fig. 1. Scanning electron microscope images of low-density samples: cellulose triacetate (TAC) (**a**) and (**b**), agar (**c**) foam polystyrene (PS) (**d**). Figures after polymer type show density in mg/cc.

https://doi.org/10.1017/S0263034608000578 Published online by Cambridge University Press

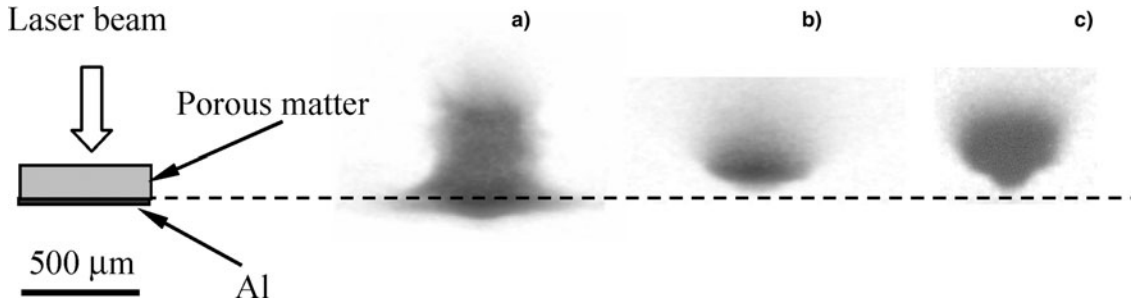

Fig. 2. X-ray pinhole images obtained in experiments on laser irradiation of low-density samples ($\rho = 10$ mg/cm^3, $d = 200$ μm): (**a**) foam polystyrene, (**b**) agar, (**c**) cellulose triacetate. The 1.5 μm-thick Al foil was placed at the rear surface of targets.

EXPERIMENTAL RESULTS AND DISCUSSION

To study the specific features of laser light absorption and energy transport in porous targets of different microstructure, the experiments were conducted on irradiation of foam polystyrene, agar, TAC samples of different average density and thickness. Figure 2 shows typical X-ray images obtained with a filtered pinhole camera (quanta energy in the range from 0.8 to 2 keV) in experiments on irradiation of 200 μm-thick polystyrene (a), agar (b), and cellulose triacetate (c) samples of the same average density (10 mg/cm^3).

As one can see in Figure 2, the extension of hot plasma region in agar and cellulose triacetate does not exceed 0.15–0.2 mm, while in polystyrene it extends over the whole porous sample thickness, and even the intense emission of Al foil placed at the target rear surface is observed. In experiments with thicker polystyrene samples, the extension of hot plasma region was ∼0.6 mm.

The information on energy transport rate inside investigated materials was obtained from results of space- and time-resolved side-on measurements of X-ray emission of high temperature plasma in porous samples, and from the measurements of target rear-surface luminosity in visible (1.5 μm-thick Al foil placed at the rear surface of investigated low-density samples prevents recording of visible light emitted from the sample interior). Typical examples of side-on X-ray recordings in experiments with agar and polystyrene targets are presented in Figure 3. As one can see, the rate of energy transport in polystyrene sample is significantly higher than that in agar sample. This conclusion agrees well with the data obtained by recording of the target rear-surface luminosity in visible. Luminosity measurements with porous samples of different thickness (200–600 μm) allowed us to estimate the velocities of heat wave front in irradiated porous materials. In polystyrene

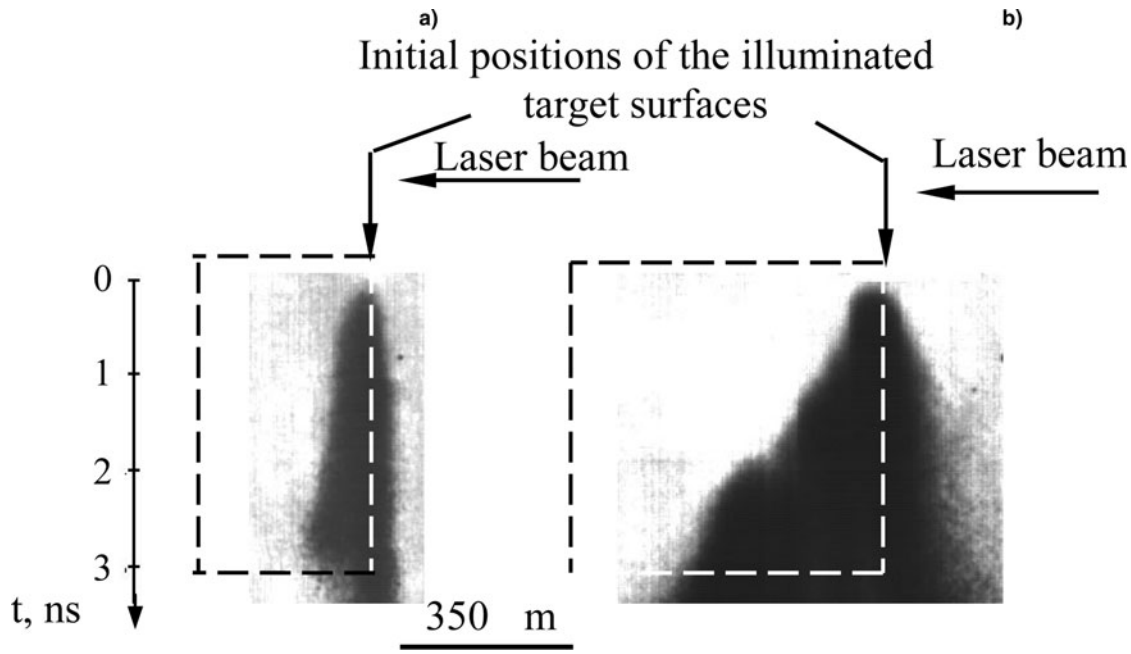

Fig. 3. Streak-camera recordings of plasma X-ray emission in experiments with targets of the same (10 mg/cm^3) average density: (**a**) agar ($d = 350$ μm), (**b**) foam polystyrene ($d = 600$ μm). Dashed lines indicate the initial positions of porous samples; $t = 0$ corresponds to the laser pulse start.

https://doi.org/10.1017/S0263034608000578 Published online by Cambridge University Press

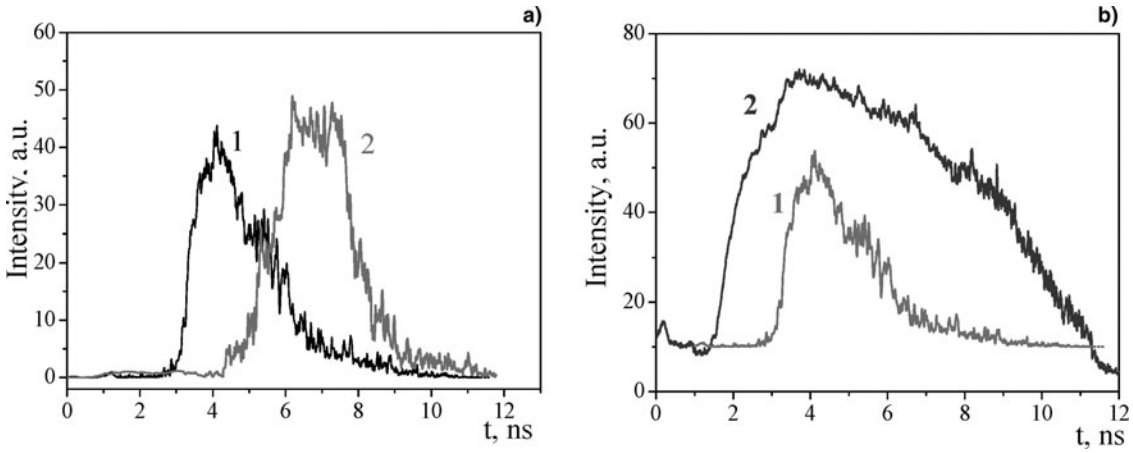

Fig. 4. Time history of the luminosity in visible at the target rear-surface ("0" corresponds to the laser pulse start). Targets: (**a**) 1 − TAC ($\rho = 10$ mg/cm^3, thickness = 200 μm), 2 − agar ($\rho = 10$ mg/cm^3, thickness = 200 μm); (**b**) 1 − TAC ($\rho = 2$ mg/cm^3, thickness = 240 μm), 2 − TAC ($\rho = 10$ mg/cm^3, thickness = 200 μm).

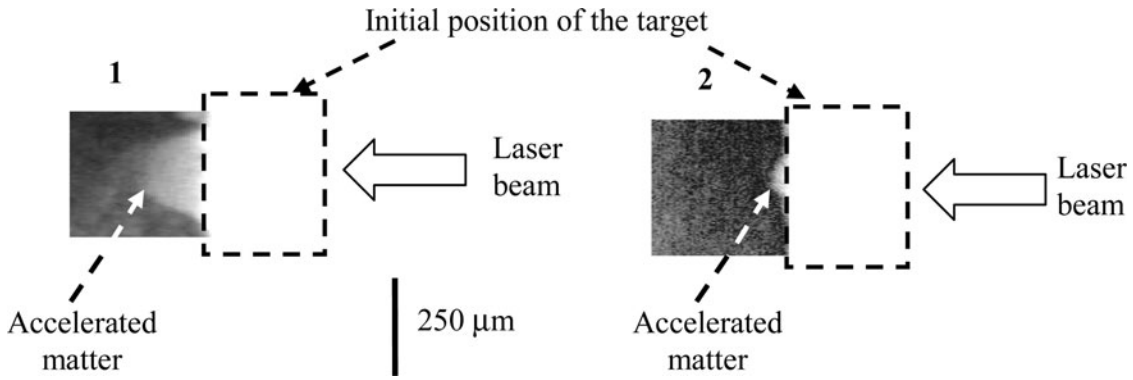

Fig. 5. Shadowgraphy frames at 7 ns after laser pulse beginning at the target rear-side: 1 − TAC, 2 − agar. Average density of samples is equal to 10 mg/cm^3, thickness −0.3 mm, $I = 5 \times 10^{13}$ W/cm^2, frame exposure −0.3 ns.

samples ($\rho = 10$ mg/cm^3) this velocity is equal to 3×10^7 cm/s, while it is a factor of four lower in agar samples of the same density (7×10^6 cm/s).

The data obtained from time-resolved measurements of plasma X-ray emission and target rear-surface luminosity in visible are confirmed by the multiframe shadowgraphy results that demonstrated Al foil dynamics at the rear-side of polystyrene and agar samples. For 200 μm-thick polystyrene sample with average density of 10 mg/cm^3, the motion of low-temperature Al plasma is observed as soon as 4 ns after laser-irradiation start. For agar sample of the same thickness and average density, the motion of Al plasma becomes noticeably much later. It should be noted that in agar targets of ∼2 mg/cm^3 average density, the longitudinal size of absorption zone and the energy transfer rate are close to those measured in experiments with foam polystyrene targets of ∼10 mg/cm^3 average density.

Now the results obtained in experiments with TAC and agar targets will be compared. The information on energy transport rate inside laser-irradiated agar and TAC samples materials was obtained from space- and time-resolved

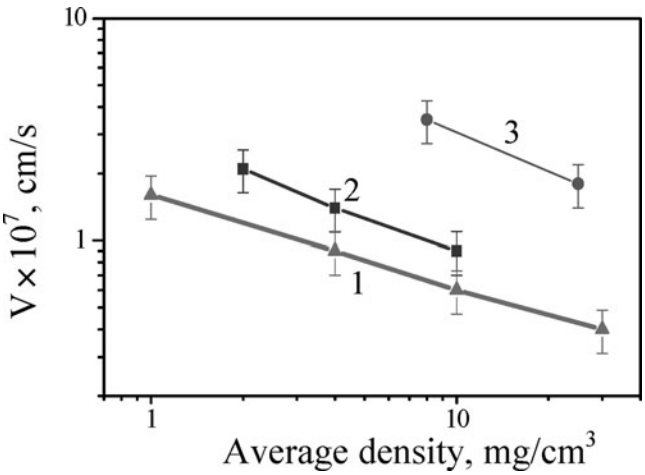

Fig. 6. Velocity of heat wave front versus porous target density: 1 – agar; 2 – TAC, 3 – foam polystyrene. $I = 5 \times 10^{13}$ W/cm^2.

https://doi.org/10.1017/S0263034608000578 Published online by Cambridge University Press

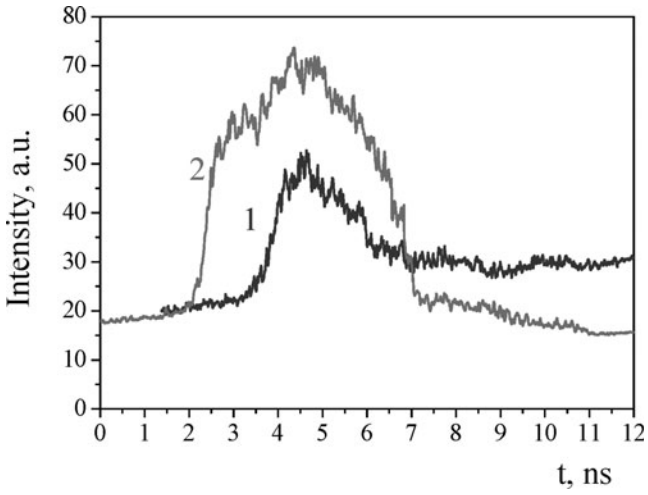

Fig. 7. Time history of the luminosity in visible at the target rear-surface ("0" corresponds to the laser pulse start). Targets: 1 – TAC ($\rho = 10$ mg/cm^3, thickness = 300 μm), 2 – TAC ($\rho = 8$ mg/cm^3, thickness = 300 μm) doped by Cu ($\rho = 2$ mg/cm^3).

measurements of the target rear-surface luminosity in visible (see Fig. 4) and multiframe shadowgraphy (see Fig. 5) (Burdonskii *et al.*, 1988; Pisarczyk *et al.*, 1994; Montgomery *et al.*, 1999). Figure 4A shows that in TAC targets, the heat front velocity is larger than that in agar targets of the same average density. The accurate values of heat wave velocities were determined from analysis of experimental data obtained in experiments with targets of different thickness. Note, that for these measurements to be correct, the thickness of samples should exceed the extension of the region where efficient absorption of laser radiation takes place (100–150 μm for $\rho = 10$ mg/cm^3). The heat wave velocities for TAC and agar targets of 10 mg/cm^3 average density were estimated as 9×10^6 cm/s and 7×10^6 cm/s, correspondingly. These values are in a good agreement with the predictions of hydrothermal wave energy transport model (Bugrov *et al.*, 1997). Remind that the velocity of heat wave front in polystyrene samples ($\rho = 10$ mg/cm^3) is as high as 3×10^7 cm/s (the accuracy of these measurements was about 15%). Figure 5 shows typical shadowgraphy frames obtained at 7 ns after laser pulse beginning in experiments on irradiation of TAC and agar samples (0.3 mm-thick, 10 mg/cm^3). One can see that in the case of TAC sample, the pronounced motion of accelerated low-temperature Al plasma takes place. For the agar sample, the displacement of Al plasma edge from the initial position of the sample rear surface is hardly observed. The shadowgraphy data acquired in experiments with TAC, agar and foam polystyrene targets show that under similar irradiation conditions and target parameters (0.3 mm, 10 mg/cm^3); the same velocity (8×10^6 cm/s) of Al plasma is realized.

Experiments with laser irradiation of TAC samples with average density of 10 mg/cm^3 and 2 mg/cm^3 (presently the lowest attainable density) were carried out also. To determine the rates of energy transport from the absorption region to the rear surface of the porous samples, the measurements of target rear-side luminosity in visible were used. The obtained data are presented in Figure 4B. The samples of different thickness (200–400 μm) were illuminated in these experiments. As a result, the measured rates of energy transport from the absorption region to the rear surface of porous TAC samples with average density of 10 mg/cm^3 and 2 mg/cm^3 were equal to $\sim 9 \times 10^6$ cm/s and $\sim 2.0 \times 10^7$ cm/s, correspondingly.

Experimentally obtained average density dependences of energy transport rate in foam polystyrene, agar, and TAC are shown in Figure 6.

Thus, all results of our experimental investigations reveal the significant difference in the processes and mechanisms responsible for the laser-light absorption, hot plasma formation, and energy transport in low-density materials of different microstructure ("open and closed cells") (Gavrilov *et al.*, 2004).

Analysis of data obtained in experiments with agar and TAC samples proves that despite of radical differences in

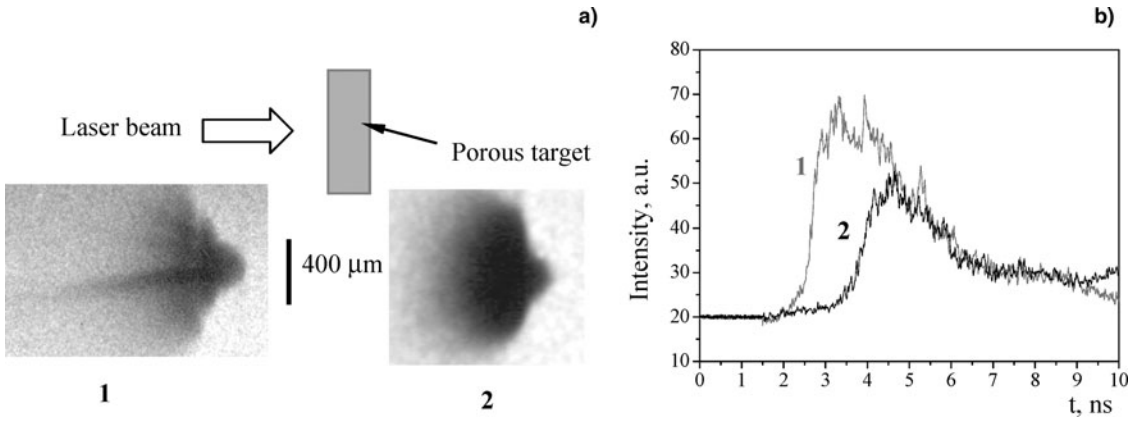

Fig. 8. (**a**) X-ray pinhole images obtained in experiments on laser irradiation of TAC samples ($\rho = 10$ mg/cm^3, $d = 300$ μm): **1** – with jets, **2** – without jets; (**b**) time history of the luminosity in visible at the target rear-surface (1 and 2, correspondingly). "0" corresponds to the laser pulse start.

https://doi.org/10.1017/S0263034608000578 Published online by Cambridge University Press

the characteristic scales of microstructure in both "open cells" porous materials the absorption efficiency and the energy-transport rate are practically undistinguished. But the higher uniformity of small-scale structure element distribution in TAC samples provides, as expected, the better reproducibility of experimental results and higher efficiency of irradiation nonuniformity smoothing.

Experiments with TAC samples doped with high-Z elements (Cu 20% admixture by weight) show that in the case of targets with average density $\sim 10\ \mathrm{mg/cm^3}$, the measured rate of energy transport from the laser light absorption region to the rear surface of irradiated sample is about 20% higher than that in undoped TAC samples (Fig. 7). Similar increase in the energy transport rate was observed in earlier experiments with Cu-doped agar samples and was explained by the essential influence of radiative wave on the energy transport process (Bugrov *et al.*, 2002, 2003).

It should be noticed that in some experiments on TAC sample irradiation, the plasma jets propagating toward laser beam are observed (Fig. 8A). In these experiments, the start of luminosity in visible at the sample rear surface caused by the heat wave arrival was recorded earlier than that in experiments without plasma jet formation (Fig. 8B).

CONCLUSIONS

New experimental results on powerful (10^{13}–$10^{14}\ \mathrm{W/cm^2}$) laser beam interaction with low-density (from $2\ \mathrm{mg/cm^3}$ to $10\ \mathrm{mg/cm^3}$) porous samples of agar, cellulose triacetate (TAC) aerogel, and foam polysterene were obtained. Agar and TAC have an "open cells" structure but structure element dimensions in agar are by an order of magnitude larger than those in TAC. Foam polysterene has a "closed cells" structure.

The pronounced effect of material microstructure onto laser-light absorption, energy transport, and parameters of produced plasma was revealed. In samples of all investigated porous materials, the absorption exhibits a volume character, and the energy transport into target interior occurs with high efficiency. However, the physical mechanisms and quantitative characteristics of these processes in "open cells" and "closed cells" materials are recognized to be quite different.

It was found that in $10\ \mathrm{mg/cm^3}$ TAC samples, the extension of hot plasma ($\sim 200\ \mu\mathrm{m}$) and energy transport rate ($\sim 9 \times 10^6\ \mathrm{cm/s}$) were close to the values measured in agar samples of the same average density ($\sim 150\ \mu\mathrm{m}$ and $\sim 7 \times 10^6\ \mathrm{cm/s}$, correspondingly). For TAC samples of the lowest attainable average density of $2\ \mathrm{mg/cm^3}$ measured energy transport rate was $\sim 2 \times 10^7\ \mathrm{cm/s}$ (in $2\ \mathrm{mg/cm^3}$ agar samples the energy transport rate was $\sim 1.5 \times 10^7\ \mathrm{cm/s}$).

In distinction to "open cells" materials in foam polysterene ($\rho = 10\ \mathrm{mg/cm^3}$), the extension of the hot plasma region was approximately $600\ \mu\mathrm{m}$ and the energy transport rate was as high as $3 \times 10^7\ \mathrm{cm/s}$.

Doping of TAC samples with high-Z element (Cu, 20% admixture by weight) results in enhancement of energy transport rate by a factor 1.2.

Small-scale structure elements in TAC samples provides the better reproducibility of experimental results as well as efficient irradiation nonuniformity smoothing because of fiber thicknesses and cell scales in agar samples (micrometers and some tens of micrometers, correspondingly) are by an order of magnitude larger than those in TAC samples.

ACKNOWLEDGMENT

This work was supported by the Russian Foundation for Basic Research (Projects No. 06-02-17526 and 08-02-00814).

REFERENCES

Bolotin, V.A., Burdonskii, I.N., Gavrilov, V.V., Goltsov, A.Yu., Kondrashov, V.N., Kovalskiy, N.G., Pergament, M.I. & Zhuzhukalo, E.V. (1992). X-ray shadowgraphy applications in ablatively accelerated planar foil studies. Studies of thin foils acceleration by pulsed laser beam. *Laser Part. Beams* **10**, 685–688.

Borisenko, N.G., Akunets, A.A., Bushuev, V.S., Dorogotovtsev, V.M. & Merkuliev, Yu.A. (2003). Motivation and fabrication methods for inertial confinement fusion energy targets. *Laser Part. Beams* **21**, 505–509.

Bugrov, A.E., Gus'kov, S.Yu., Rozanov, V.B., Burdonskii, I.N., Gavrilov, V.V., Goltsov, A.Yu., Zhuzhukalo, E.V. V.N., Kovalskii, N.G., Pergament, M.I. & Petryakov, V.M. (1997). Interaction of a high-power laser beam with low-density porous media. *JETP* **84**, 497–506.

Bugrov, A.E., Burdonskii, I.N., Gavrilov, V.V., Goltsov, A.Yu., Gus'kov, S.Yu., Zhuzhukalo, E.V., Kovalskii, N.G., Kondrashov, V.N., Pergament, M.I., Petryakov, V.M., Rozanov, V.B. & Tzoi, S.D. (1999*a*). Absorption and scattering of high-power laser radiation in low-density porous media. *JETP* **88**, 441–448.

Bugrov, A.E., Burdonskii, I.N., Gavrilov, V.V., Goltsov, A.Yu., Gus'kov, S.Yu., Kondrashov, V.N., Kovalskiy, N.G., Medovshchikov, S.F., Pergament, M.I., Petryakov, V.M., Rozanov, V.B. & Zhuzhukalo, E.V. (1999*b*). Investigation of light absorption, energy transfer and plasma dynamic processes in laser-irradiated targets of low average density. *Laser Part. Beams* **17**, 415–426.

Bugrov, A.E., Burdonskii, I.N., Gavrilov, V.V., Goltsov, A.Yu., Gus'kov, S.Yu., Kondrashov, V.N., Kovalskiy, N.G., Medovshchikov, S.F., Pergament, M.I., Petryakov, V.M., Rozanov, V.B. & Zhuzhukalo, E.V. (2000). Interaction of powerful laser and X-ray pulses with porous materials for advanced ICF targets applications. In *Inertial Fusion Sciences and Applications*, pp. 154–157, Paris, France: Elsevier.

Bugrov, A.E., Burdonskiy, I.N., Gavrilov, V.V., Goltsov, A.Yu, Gus'kov, S.Yu., Kondrashov, V.N., Koptyaev, S.N., Kovalskiy, N.G., Medovshchikov, S.F., Nikolaevskiy, V.G., Pergament, M.I., Petryakov, V.M., Rozanov, V.B., Sorokin, A.A. & Zhuzhukalo, E.V. (2001). Study of lateral heat transfer and pressure profile smoothing in laser-irradiated low-density targets. *Proc. SPIE* **4424**, 367–370.

Bugrov, A.E., Burdonskii, I.N., Gavrilov, V.V., Goltsov, S.Yu., Kondrashov, V.N., Kovalskiy, N.G., Medovshchikov, S.F., Pergament, M.I., Petryakov, V.M. & Zhuzhukalo, E.V. (2002). Characterization of laser-produced plasma and interaction processes in experiments with porous low-density targets. In *Inertial Fusion Sciences and Applications 2001*, pp. 286–290, Paris, France: Elsevier.

Bugrov, A.E., Burdonskiy, I.N., Fasakhov, I.K., Gavrilov, V.V., Goltsov, A.Yu, Gromov, A.I., Kondrashov, V.N., Kovalskiy, N.G., Medovshchikov, S.F., Nikolaevskiy, V.G., Petryakov, V.M. & Zhuzhukalo, E.V. (2003). Laser-plasma interaction in experiments with low-density volume-structured media on the "Mishen" facility. *Proc. SPIE* **5228**, 8–15.

Bugrov, A.E., Burdonskiy, I.N., Borisenko, N.G., Dimitrenko, V.V., Fasakhov, I.K., Gavrilov, V.V., Goltsov, A.Yu, Gromov, A.I., Khalenkov, A.M., Kondrashov, V.N., Kovalskii, N.G., Medovshchikov, S.F., Merkuliev, Yu.A. & Zhuzhukalo, E.V. (2006). Study of physical processes in laser-irradiated porous targets of different microstructure. *J. de Physique IV* **133**, 343–346.

Burdonskii, I.N., Velikovich, A.L., Gavrilov, V.V., Goltsov, A.Yu., Kovalskiy, N.G., Liberman, M.A., Pergament, M.I. & Zhuzhukalo, E.V. (1988). Studies of thin foils acceleration by pulsed laser beam. *Laser Part. Beams* **6**, 327–334.

Drake, R.P., Carroll, J.J., Smith, T.B., Keiter, P., Glendinning, S.G., Hurricane, O., Estabrook, K., Ryutov, D.D., Remington, B.A., Wallace, R.J., Michael, E. & Mcray, R. (2000). Laser experiments to simulate supernova remmants. *Phys. Plasmas* **7**, 2142–2148.

Gavrilov, V.V., Goltsov, A.Yu, Gus'kov, S.Yu., Demchenko, N.N., Kondrashov, V.N., Kovalskii, N.G., Rozanov, V.B., Stepanov, R.V., Yankovskii, G.M. & Zmitrenko, N.V. (2004). Experimental and numerical modeling of laser interaction with low-density porous media. *Proc. XXVIII European Conference on Laser Interaction with Matter*, pp. 322–336, Roma, Italy.

Gromov, A.I., Borisenko, N.G., Gus'kov, S.Y., Merkul'ev, Yu.A. & Mitrofanov, A.V. (1999). Fabrication and monitoring of advanced low-density media for ICF targets. *Laser Part. Beams* **17**, 661–670.

Gus'kov, S.Yu., Rozanov, V.B. & Zmitrenko, N.V. (1995). Thermonuclear "Laser green house" target with distributed absorption of laser energy. *JETP* **81**, 296–305.

Hora, H. (2007). New aspects for fusion energy using inertial confinement. *Laser Part. Beams* **25**, 37–45.

Hoffmann, D.H.H., Blazevic, A., Ni, P., Rosmej, O., Roth, M., Tahir, N.A., Tauschwitz, A., Udrea, S., Varentsov, D., Weyrich, K. & Maron, Y. (2005). Present and future perspectives for high energy density physics with intense heavy ion and laser beams. *Laser Part. Beams* **23**, 47–53.

Jungwirth, K. (2005). Recent highlights of the PALS research program. *Laser Part. Beams* **23**, 396–396.

Khalenkov, A.M., Borisenko, N.G., Kondrashov, V.N., Merkuliev, Y.A., Limpouch, J. & Pimenov, V.G. (2006). Experience of micro-heterogeneous target fabrication to study energy transport in plasma near critical density. *Laser Part. Beams* **24**, 283–290.

Koenig, M., Benuzzi, A., Philippe, F., Batani, D., Hall, T., Grandjouan, N. & Nazarov, W. (1999). Equation of state data experiments for plastic foams using smoothed laser beams. *Phys. Plasmas* **6**, 3296–3301.

Koresheva, E.R., Osipov, I.E. & Aleksandrova, I.V. (2005). Free standing target technologies for inertial fusion energy: Target fabrication, characterization, and delivery. *Laser Part. Beams* **23**, 563–571.

Landen, O.L., Farley, D.R., Glendinning, S.G., Logory, L.M., Bell, P.M., Koch, Lee, F.D., Bradley, D.K., Kalantr, Back, C.F. & Turner, R.E. (2001). X-ray backlighting for the National Ignition Facility. *Rev. Sci. Instr.* **72**, 627–634.

Lindl, J. (1995). Development of the indirect-drive approach to inertial confinement fusion and the target physics basis for ignition and gain. *Phys. Plasmas* **2**, 3933–4023.

Montgomery, D.S., Johnson, R.P., Cobble, J.A., Fernandez, J.C., Lindman, E.L., Rose, H.A. & Estebrook, K.G. (1999). Characterization of plasma and laser conditions for single hot spot experiments. *Laser Part. Beams* **17**, 349–359.

Mulser, P. & Schneider, R. (2004). On the inefficiency of hole boring in fast ignition. *Laser Part. Beams* **22**, 157–162.

Pisarczyk, T., Arendzikowski, R., Parys, P. & Patron, Z. (1994). Polari-interferometer with automatic images processing for laser plasma diagnostics. *Laser Part. Beams* **12**, 549–563.

Riley, D., Khattak, F.Y., Saiz, E.G., Gregori, G., Bandyopadhyay, S., Notley, M., Neely, D., Chambers, D., Moore, A. & Comley, A. (2007). Spectrally resolved X-ray scatter from laser-shock-driven plasmas. *Laser Part. Beams* **25**, 465–469.

Schollmeier, M., Prieto, G.R., Rosmej, F.B., Schaumann, G., Blazevic, A., Rosmej, O.N. & Roth, M. (2006). Investigation of laser-produced chlorine plasma radiation for non-monochromatic X-ray scattering experiments. *Laser Part. Beams* **24**, 335–345.

Vatulin, V.V., Kunin, A.V., Golubev, A.A., Luk'yashin, V.E., Turtikov, V.I., Sharkov, B.Y., Baldina, E.G., Borisenko, N.G., Gnutov, A.S., Visar, J., Hoffmann, D. & Jacobi, J. (2004). Measurement of the total range and specific energy deposition of a beam of uranium ions in porous carbon targets. *At. Energy* **96**, 275–281.